AIP | Applied Physics Letters

Room-temperature quantum-dot-like luminescence from site-controlled InGaN quantum disks

L. K. Lee, Lei Zhang, Hui Deng, and P.-C. Ku

Citation: Appl. Phys. Lett. **99**, 263105 (2011); doi: 10.1063/1.3672441
View online: http://dx.doi.org/10.1063/1.3672441
View Table of Contents: http://apl.aip.org/resource/1/APPLAB/v99/i26
Published by the AIP Publishing LLC.

Room-temperature quantum-dot-like luminescence from site-controlled InGaN quantum disks

L. K. Lee,[1] Lei Zhang,[2] Hui Deng,[2] and P.-C. Ku[1,a)]
[1]*Department of Electrical Engineering and Computer Science, University of Michigan, 1301 Beal Ave., Ann Arbor, Michigan 48109, USA*
[2]*Department of Physics, University of Michigan, 450 Church St., Ann Arbor, Michigan 48109, USA*

(Received 22 July 2011; accepted 2 December 2011; published online 28 December 2011)

We studied the optical properties of site-controlled InGaN quantum disks fabricated by the top-down approach. Room-temperature quantum-dot-like photoluminescence was observed from a single InGaN quantum disk. Size-dependent emission wavelength shift was measured and attributed to the quantum confinement in the disk plane. Theoretical modeling was carried out to explain the large blue shift due to size quantization. Temperature dependent luminescence was characterized and showed an abnormally large linewidth at low temperature and a linewidth saturation above 100 K. A sidewall charge center model was proposed to explain these phenomena. © *2011 American Institute of Physics*. [doi:10.1063/1.3672441]

Since the conceptualization of semiconductor quantum dots (QDs) nearly three decades ago,[1,2] these man-made nanostructures have been regarded as one of the most promising route for solid-state devices to fully exploit quantum optical effects.[3] Indeed, semiconductors based photon-on-demand sources, one-atom lasers, and single-quantum-dot polariton lasers have been proposed, demonstrated, and extensively studied.[4–11] In spite of these advances, the road to practical, large-scale applications of these phenomena and devices are still impeded by two serious challenges, namely, the control of QD positions and their emission wavelength, and the preservation of their unique luminescence properties at a technologically relevant temperature, often the room temperature. III-nitride QDs exhibit large exciton binding energy ($\geq$26 meV), large oscillator strength, and their heterostructures' band offsets are among the largest in compound semiconductors, making them one of the best candidates to the realize high-temperature quantum optical devices. To this end, developing III-nitride QDs with precisely controlled positions and emission wavelengths that can operate at room temperature is a crucial step toward this goal. In this paper, we report the observation of room-temperature quantum-dot-like luminescence from a single site-controlled InGaN/GaN quantum disk. We demonstrated that the top-down approach is feasible in the synthesis of high-quality group-III nitride QD materials. Our fabrication methodology is simple and scalable, allowing further improvements in the control of optical properties to be possible. The results can provide a new opportunity for the realization of scalable room-temperature semiconductor quantum light sources.

Recently, we showed that high-quality site-controlled InGaN/GaN quantum disk structures can be obtained by using a top-down approach which involves inductively coupled plasma reactive-ion etching (ICP-RIE) and atomic-layer deposition (ALD).[12] A single InGaN/GaN quantum well (QW) sample was patterned into an array of nanoscale pillars with a height of 120 nm using ICP-RIE, and encapsulated by 40-nm thick Al_2O_3 using ALD. The InGaN region forms a nanoscale disk that is surrounded by 10-nm thick uid-GaN (unintentionally doped GaN) on the top, Al_2O_3 on the side, and uid-GaN on the bottom. More details on the sample preparation can be found in Ref. 12. In this paper, we focus on the optical properties of the single InGaN/GaN quantum disk.

Single-disk spectroscopy was carried out using a micro-photoluminescence (μ-PL) setup equipped with a 50$\times$ objective lens, responsible for both excitation and signal collection. The 390-nm wavelength ultrashort-pulsed laser excitation (from the second-harmonic output of a mode-locked Ti:sapphire laser with a pulse width of 130 fs) was focused down to a beam spot of 2 μm diameter, giving an excitation intensity of 5 kW/cm^2. PL signal was acquired by a photomultiplier tube (PMT) and a monochromator with 50-cm focal length, providing an overall spectral resolution of 1 Å. The excitation was tuned to be below the GaN bandgap such that no measurable luminescence was from the GaN background that would interfere with the measurement. Figure 1(a) shows a single nanopillar consisting of a 17-nm-diameter (measured at the InGaN plane using scanning electron microscopy (SEM)), 3-nm-height InGaN quantum disk located at the center of a $100 \times 100\ \mu m^2$ area where no other InGaN structures exist. The measured single-disk PL is plotted in Fig. 1(c). We compared the measured PL with the calculated spontaneous emission spectra from both a single QD and a QW. In the case of QD calculations, we assumed a Lorentzian line-shape linewidth broadening with the linewidth and peak intensity being the only fitting parameters. In the case of the QW, an additional fitting parameter, the carrier concentration, was used. As a comparison, we also plotted the PL measured from the unetched QW of the same sample. For convenience of comparison, we have normalized the spectrum and shifted the peak photon energy to that of the single-disk emission. All results are shown together with the single-dot PL in Fig. 1(c). It is evident that the measured single-disk spectrum agrees well with the calculated QD emission but not the QW emission, calculated or measured. The QW PL exhibits a clear high-energy tail which is attributed to the integration of the QW density-of-state (DOS) and

a)Electronic mail: peicheng@umich.edu.

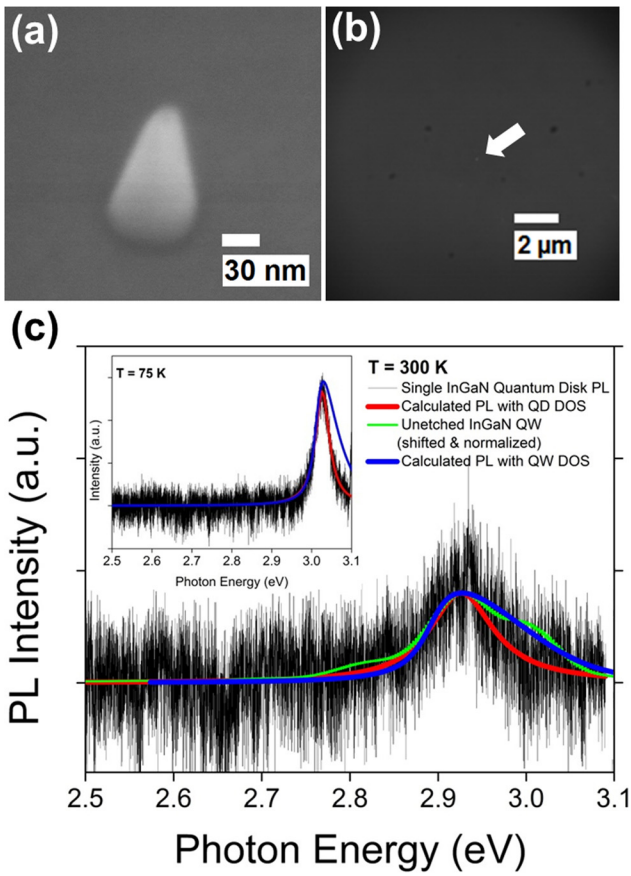

FIG. 1. (Color online) (a) The SEM image of a single site-controlled InGaN quantum disk of a diameter of 17 nm. (b) CCD image of a single quantum disk emission at room-temperature. (c) Room temperature PL spectrum of a single quantum disk compared to unetched QW (measured) as well as calculated QD and QW emission. The inset shows the same comparison at 75 K.

the Fermi-Dirac distribution of the carriers. To see more contrast in this comparison, in the inset of Fig. 1(c), we show the measured and calculated PL spectra of the same quantum disk at 75 K, where the PL signal is stronger and more distinct. All the spectra preserve the same features as described above, with the spectrum calculated using the QD DOS

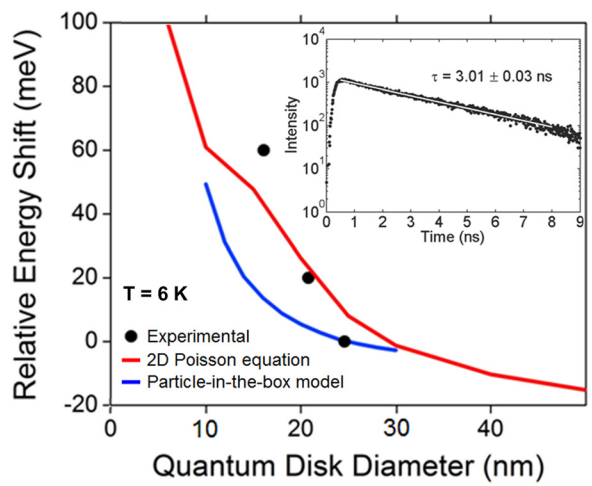

FIG. 2. (Color online) The relative peak emission wavelength of single InGaN quantum disks with diameters of 16, 21, and 25 nm as compared to two different models: the particle-in-the-box model and the model used in this work (2D Poisson equation). The inset shows the time-resolved photoluminescence trace of a 15-nm diameter dot measured at 6 K. The straight line corresponds to a single exponential lifetime of 3.01 ns.

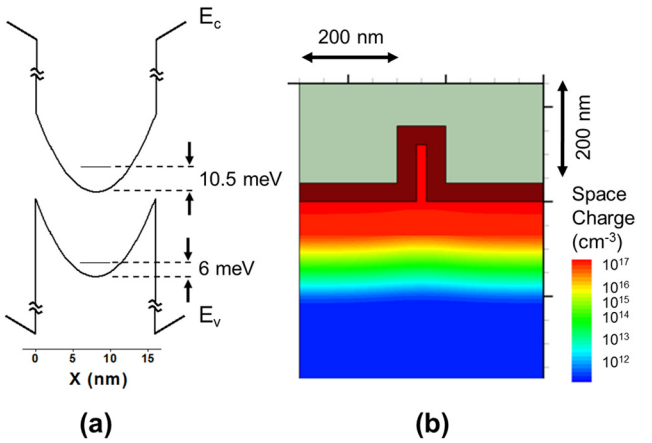

FIG. 3. (Color online) (a) The calculated band diagram of a 16-nm-diameter, fully depleted pillar, and the ground conduction and valence band states. (b) The calculated space charge density distribution of a 20-nm-diameter nanopillar with a doping concentration of $10^{17}\,cm^{-3}$ (n-type) covered by a 40-nm-thick Al_2O_3 layer.

agrees better with the experimental data. We, therefore, conclude that the quantum disk has emission characteristics closer to a QD than to a QW.

In semiconductor QDs, carriers are locally confined in all three dimensions. Therefore, the emission wavelength of a QD can be controlled by changing its dimension in any direction. A smaller dot size will cause a larger separation of electron and hole ground state energies and results in a blue-shift of emission energy. To characterize such an effect in the single InGaN quantum disk, we measured the emission wavelength for quantum disks of different diameters: 16 nm, 21 nm, and 25 nm. The results are shown in Fig. 2. As the diameter of the quantum disk becomes smaller, the emission wavelength is blue-shifted, as a result of the quantum confinement in the disk plane. This is further confirmed by the mono-exponential time-resolved PL trace shown in the inset.

We theoretically calculated the amount of blue shift due to size quantization. We noted that the simple particle-in-the-box model, i.e., assuming an infinite square-well potential profile, cannot fully account for the amount of energy shift observed in the experiment. Although previous studies have shown that the formation of InGaN nanopillars by etching resulted in a blue-shift in the emission wavelength due to the strain relaxation in the nanopillar which led to the reduction of the quantum-confined Stark effect (QCSE), the amount of shift became too small at the small dimension in the current case and failed to explain our observation.[13,14] In our sample, the emission energy of the unetched QW at the same temperature is 2.854 eV. The average emission energy of the disks of 16–25 nm diameter is 2.947 eV. Hence, the blue shift from the 8-nm range of diameter variation is already comparable to the total amount of shift that can be attributed to the strain relaxation. In order to explain the large blue shift in Fig. 2, we calculated the energy band edge profile of the nanopillar using Synopsys Sentaurus TCAD. For simplicity, we neglected the piezoelectric field along the c-axis as we were mainly concerned with the band edge in the disk plane. We also assumed the doping concentration in our uid-GaN was $10^{17}\,cm^{-3}$ and was n-type.[15] The result is shown in Fig. 3. It can be seen that the entire nanopillar is

depleted as the space-charge density equals the doping density, and thus, the band bending occurs towards the sidewall of the nanopillar. As the nanopillar diameter becomes smaller, the bending permeates throughout the entire disk plane, significantly changing the eigen-state energies. By numerically solving the Schrödinger's equation using the band edge profile in the InGaN plane while neglecting the influence of the potential profile in the substrate normal direction, the emission wavelength versus disk diameter is plotted in Fig. 2, showing a much better agreement with the experimental results.

The temperature dependence of the single-disk PL was also characterized. The results are summarized in Fig. 4 for emission wavelength (Fig. 4(a)), integrated PL intensity (Fig. 4(a) inset), and FWHM linewidth (Fig. 4(b)). In contrast to the typical s-shaped temperature dependence as observed in InGaN quantum wells,[16] the emission wavelength fits relatively well with the Varshni's model $E(T) = E_0(T) - \alpha T^2/(\beta + T)$ with $\alpha = 8.54 \times 10^{-4}$ eV/K and $\beta = 550$ K, which is attributed to the reduced piezoelectric field and localized carrier confinement in the quantum disk. The Arrhenius plot (Fig. 4(a) inset) shows a 33% radiative efficiency at room temperature. The high radiative efficiency is attributed to the carrier confinement in the disk plane and conformal passivation of the Al_2O_3 layer by ALD which was also evidenced by the negligible yellow band luminescence (YBL).[12] The FWHM linewidth shows some interesting behaviors. First, the low temperature linewidth (24 meV) is comparable to that of a GaN/AlN quantum dot grown by the Stranski-Krastanov (SK) mechanism,[5] but is much broader than some reported values of only 100 μeV from the InGaN QDs, also grown by the SK mode.[17–20] We attributed the wide range and sometimes abnormally large linewidth values in these III-nitride materials to the piezoelectric field and the associated spectral diffusion.[5,21–23] In our quantum disk, an additional electric field exists in the disk plane as discussed above due to depletion of the nanopillar. Hence, any random charge trapping and release from the nearby defect or surface states can cause a large fluctuation of the emission wavelength. Below 100 K, the data in Fig. 4(b) can be fitted with the typical linewidth equation used for the quantum dot as follows:

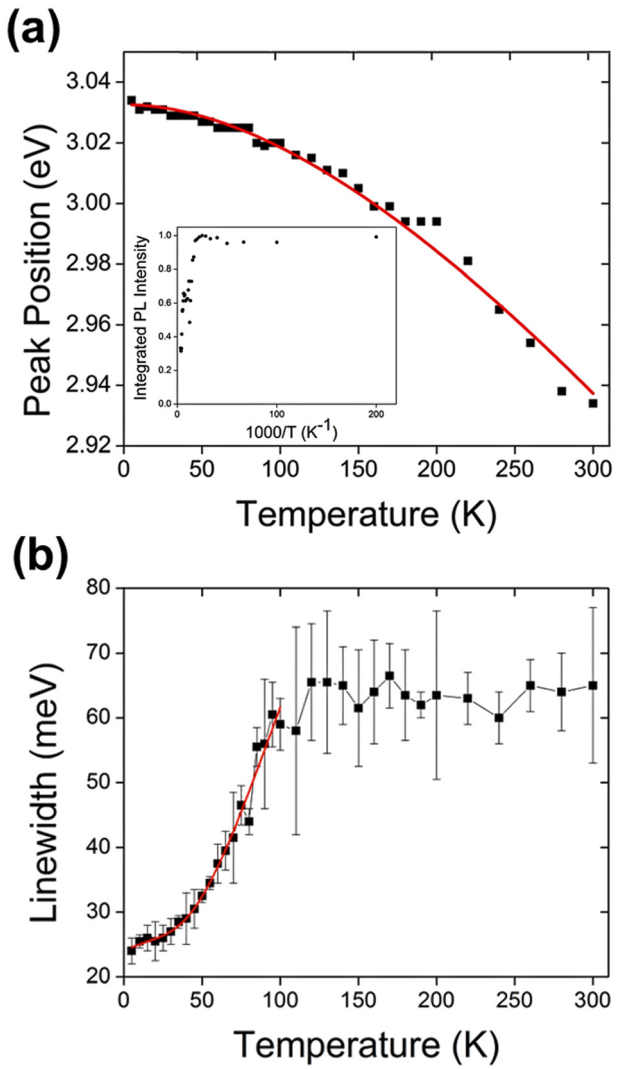

FIG. 4. (Color online) (a) The measured peak emission energy versus temperature (squares) and the fitting by Varshni's model (solid line). Inset shows the Arrhenius plot of the integrated PL intensity. (b) FWHM linewidth versus temperature (squares) and the fitting based on Eq. (1) (red line).

$$\Gamma(T) = \Gamma_0 + \gamma_p T + \gamma_a \exp(-E_a/k_B T), \quad (1)$$

where Γ_0 is the FWHM linewidth at 0 K, γ_p is the coefficient for coupling to acoustic phonons, γ_a is the coefficient for the exponential term that describes the activation of carriers over an energy barrier E_a, leaving the localization potential. The fitting gives $\gamma_p = 87 \pm 70$ μeV, $\gamma_a = 211 \pm 52$ meV, and $E_a = 17 \pm 3$ meV. The activation energy E_a obtained from fitting is comparable to previous findings. However, above 100 K, the linewidth seems to be saturated and the data can no longer be fitted by Eq. (1) regardless of the fitting parameters. To explain the discrepancy to Eq. (1), we propose a sidewall charge center (SCC) model. Surface and defects states such as gallium vacancies are inevitable on the nanopillar sidewalls. These SCC states can act as charge trapping centers which may randomly and repeatedly capture and release carriers generated in the nanopillars. Due to the band bending of the valence band edge towards the sidewall (Fig. 3), trapping of the carrier by the SCC states can compete effectively with the radiative process near the center of the quantum disk. As the temperature increases, the nonradiative recombination rate in these SCC states increases, making more SCC states available to compete for the carriers in the quantum disk and, therefore, reducing the exciton lifetime and resulting in the broadening of the emission linewidth. Since the surface area around the InGaN quantum disk and, therefore, the total number of the SCC states available are finite, when the number of the available SCC states no longer increases with the temperature, the emission linewidth of the quantum disk saturates. The random capture and release of the carriers from these SCC states can also attribute to the abnormally large emission linewidth at low temperature via spectral diffusion which agrees with previously reported data.

In summary, room-temperature quantum-dot-like luminescence was observed from a site-controlled InGaN quantum disk. The quantum disk is embedded in a nanopillar and

is passivated by an Al_2O_3 layer. The fabrication procedure is simple and scalable, involving only ICP-RIE and ALD. Using μ-PL, we studied the optical properties of the single InGaN quantum disk and compared the results with theoretical modeling. The single-disk PL fitted well with the calculated emission from a single QD. The wavelength tuning due to quantum confinement was also observed and modeled. The results showed the importance of the band edge shape on the emission wavelength. The temperature-dependent PL measurement showed a lessened effect from the piezoelectric effect as well as a high radiative efficiency at room temperature, both being attributed to carrier confinement and reduced piezoelectric field in the InGaN layer. The emission linewidth of the single disk was found to be profoundly influenced by the internal electric field present in all directions of the quantum disk, resulting in abnormally large linewidth at low temperature and a saturated linewidth above 100 K.

Optical measurements in this work were supported as part of the Center for Solar and Thermal Energy Conversion, an Energy Frontier Research Center funded by the U.S. Department of Energy, Office of Science, Office of Basic Energy Sciences under Award No. DE-SC0000957. Theoretical modeling was supported by the National Science Foundation (under Grants ECCS No. 0901477 and ECCS No. 1102127). Synthesis was supported by the Defense Advanced Research Project Agency (DARPA) under Grant No. N66001-10-1-4042 and was performed in Lurie Nanofabrication Facility which is a part of the NSF NNIN network.

[1]Y. Arakawa and H. Sakaki, Appl. Phys. Lett. **40**, 939 (1982).
[2]U. Banin, Y. Cao, D. Katz, and O. Millo, Nature **400**, 542 (1999).
[3]A. J. Shields, Nature Photon. **1**, 215 (2007).
[4]C. Santori, D. Fattal, J. Vučković, G. S. Solomon, and Y. Yamamoto, Nature **419**, 594 (2002).
[5]S. Kako, C. Santori, K. Hoshino, S. Götzinger, Y. Yamamoto, and Y. Arakawa, Nature Mater. **5**, 887 (2006).
[6]G. Khitrova, H. M. Gibbs, M. Kira, S. W. Koch, and A. Scherer, Nat. Phys. **2**, 81 (2006).
[7]K. Hennessy, A. Badolato, M. Winger, D. Gerace, M. Atatüre, S. Gulde, S. Fält, E. L. Hu, and A. Imamoğlu, Nature **445**, 896 (2007).
[8]P. Gallo, M. Felici, B. Dwir, K. A. Atlasov, K. F. Karlsson, A. Rudra, A. Mohan, G. Biasiol, L. Sorba, and E. Kapon, Appl. Phys. Lett. **92**, 263101 (2008).
[9]C. Schneider, T. Heindel, A. Huggenberger, P. Weinmann, C. Kistner, M. Kamp, S. Reitzenstein, S. Höfling, and A. Forchel, Appl. Phys. Lett. **94**, 111111 (2009).
[10]M. Nomura, N. Kumagai, S. Iwamoto, Y. Ota, and Y. Arakawa, Nat. Phys. **6**, 279 (2010).
[11]J. Heinrich, A. Huggenberger, T. Heindel, S. Reitzenstein, S. Höfling, L. Worschech, and A. Forchel, Appl. Phys. Lett. **96**, 211117 (2010).
[12]L. K. Lee and P.-C. Ku, "Fabrication of site-controlled InGaN quantum dots using reactive-ion etching," Physica Status Solidi C (to be published).
[13]P. Yu, C. H. Chiu, Y.-R. Wu, H. H. Yen, J. R. Chen, C. C. Kao, H.-W. Yang, H. C. Kuo, T. C. Lu, W. Y. Yeh *et al.*, Appl. Phys. Lett. **93**, 081110 (2008).
[14]V. Ramesh, A. Kikuchi, K. Kishino, M. Funato, and Y. Kawakami, J. Appl. Phys. **107**, 114303 (2010).
[15]P. Bogusławski, E. L. Briggs, and J. Bernholc, Phys. Rev. B **51**, 17255 (1995).
[16]Y.-H. Cho, G. H. Gainer, A. J. Fischer, J. J. Song, S. Keller, U. K. Mishra, and S. P. DenBaars, Appl. Phys. Lett. **73**, 1370 (1998).
[17]R. Seguin, S. Rodt, A. Strittmatter, L. Reißmann, T. Bartel, A. Hoffmann, D. Bimberg, E. Hahn, and D. Gerthsen, Appl. Phys. Lett. **84**, 4023 (2004).
[18]J. H. Rice, J. W. Robinson, J. D. Smith, A. Jarjour, R. A. Taylor, R. A. Oliver, G. Andrew, D. Briggs, M. J. Kappers, S. Yasin *et al.*, IEEE Trans. Nanotechnol. **3**, 343 (2004).
[19]H. Schömig, S. Halm, A. Forchel, G. Bacher, J. Off, and F. Scholz, Phys. Rev. Lett. **92**, 106802 (2004).
[20]K. Sebald, H. Lohmeyer, J. Gutowski, T. Yamaguchi, and D. Hommel, Phys. Status Solidi B **243**, 1661 (2006).
[21]S. A. Empedocles and M. G. Bawendi, Science **278**, 2114 (1997).
[22]S. Kako, K. Hoshino, S. Iwamoto, S. Ishida, and Y. Arakawa, Appl. Phys. Lett. **85**, 64 (2004).
[23]J. H. Rice, J. W. Robinson, A. Jarjour, R. A. Taylor, R. A. Oliver, G. Andrew, D. Briggs, M. J. Kappers, and C. J. Humphreys, Appl. Phys. Lett. **84**, 4110 (2004).